



# Expanded CUG Repeat RNA Induces Premature Senescence in Myotonic Dystrophy Model Cells

Yuhei Hasuike, Hideki Mochizuki and Masayuki Nakamori\*

Department of Neurology, Osaka University Graduate School of Medicine, Osaka, Japan

Myotonic dystrophy type 1 (DM1) is a dominantly inherited disorder due to a toxic gain of function of RNA transcripts containing expanded CUG repeats (CUG<sup>exp</sup>). Patients with DM1 present with multisystemic symptoms, such as muscle wasting, cognitive impairment, cataract, frontal baldness, and endocrine defects, which resemble accelerated aging. Although the involvement of cellular senescence, a critical component of aging, was suggested in studies of DM1 patient-derived cells, the detailed mechanism of cellular senescence caused by CUG<sup>exp</sup> RNA remains unelucidated. Here, we developed a DM1 cell model that conditionally expressed CUG<sup>exp</sup> RNA in human primary cells so that we could perform a detailed assessment that eliminated the variability in primary cells from different origins. Our DM1 model cells demonstrated that CUG<sup>exp</sup> RNA expression induced cellular senescence by a telomere-independent mechanism. Furthermore, the toxic RNA expression caused mitochondrial dysfunction, excessive reactive oxygen species production, and DNA damage and response, resulting in the senescence-associated increase of cell cycle inhibitors p21 and p16 and secreted mediators insulin-like growth factor binding protein 3 (IGFBP3) and plasminogen activator inhibitor-1 (PAI-1). This study provides unequivocal evidence of the induction of premature senescence by CUG<sup>exp</sup> RNA in our DM1 model cells.

**Keywords:** IGFBP3, PAI-1, repeat expansion, cellular senescence, reactive oxygen species, myotonic dystrophy

## OPEN ACCESS

### Edited by:

Giovanni Meola,  
University of Milan, Italy

### Reviewed by:

Mani Mahadevan,  
University of Virginia, United States  
Tohru Matsuura,  
Jichi Medical University, Japan

### \*Correspondence:

Masayuki Nakamori  
mnakamor@neuro.med.osaka-  
u.ac.jp

### Specialty section:

This article was submitted to  
Neurogenomics,  
a section of the journal  
Frontiers in Genetics

**Received:** 30 January 2022

**Accepted:** 11 March 2022

**Published:** 25 March 2022

### Citation:

Hasuike Y, Mochizuki H and  
Nakamori M (2022) Expanded CUG  
Repeat RNA Induces Premature  
Senescence in Myotonic Dystrophy  
Model Cells.  
Front. Genet. 13:865811.  
doi: 10.3389/fgene.2022.865811

## INTRODUCTION

Myotonic dystrophy type 1 (DM1, OMIM #160900) is the most common form of muscular dystrophy in adults (Johnson et al., 2021). The clinical manifestations of DM1 are characterized by multisystemic symptoms, including muscle wasting, myotonia, cardiac conduction defects, cataracts, frontal balding, cognitive impairment, and endocrine defects (Thornton, 2014; Meola and Cardani, 2015). DM1 is caused by the expansion of CTG repeats in the 3'-untranslated region (UTR) of *DMPK* (Brook et al., 1992; Fu et al., 1992; Mahadevan et al., 1992). The RNA expressed from the mutant allele exerts a toxic gain of function due to the presence of an expanded CUG repeat (CUG<sup>exp</sup>), which forms ribonuclear foci in the nucleus and disrupts the regulation of alternative splicing by affecting several RNA-binding factors, including muscleblind-like splicing regulator one and CUGBP Elav-like family member one proteins (Lee and Cooper, 2009). Aberrant splicing events in *CLCN1*, *SCN5A*, and *INSR* have been associated with myotonia, arrhythmias, and insulin resistance, respectively, in DM1 (Savkur et al., 2001; Charlet et al., 2002; Freyermuth et al., 2016). However, although more than hundreds of mis-splicing events have been identified in DM1 tissues (Nakamori et al., 2013; Freyermuth et al., 2016; Otero et al., 2021), the aberrant splicing

events responsible for many multisystemic DM1 symptoms remain unclear, suggesting the involvement of additional factors in DM1 pathogenesis.

Some of the multisystemic symptoms in DM1, such as muscle wasting, cataract, cognitive impairment, and frontal baldness, resemble the appearance of accelerated aging (Meinke et al., 2018). Cellular senescence is a crucial driver of the aging process and is defined as a state of irreversible cell cycle arrest induced by stress or specific physiological processes, such as telomere erosion, oncogene overexpression, oxidative stress, mitochondrial dysfunction, and inflammation (Hernandez-Segura et al., 2018; Di Micco et al., 2021). It is characterized by morphological and metabolic changes, chromatin reorganization, and a senescence-associated secretory phenotype (SASP) (McHugh and Gil, 2018). Several studies have shown that DM1 patient-derived cells reduce proliferative capacity and induce cellular senescence (Furling et al., 2001; Bigot et al., 2009; Thornell et al., 2009; Renna et al., 2014). Other studies have suggested the involvement of oxidative stress and mitochondrial dysfunction in DM1 pathogenesis (Sahashi et al., 1992; Usuki and Ishiura, 1998; Siciliano et al., 2001; Toscano et al., 2005; Garcia-Puga et al., 2020). However, the mechanism of cellular senescence in DM1 remains still unclear, because of the limitations in assessing cellular senescence in human primary cells. The characteristics of patient-derived cells vary considerably in different genetic and environmental backgrounds (Chang et al., 2002; Maier and Westendorp, 2009; Dolivo et al., 2016). Furthermore, the proliferative lifespan of human primary cells depends on the donor's age (Kaji et al., 2009). In this study, we developed a cell model of DM1 conditionally expressing abnormal RNA containing CUG<sup>exp</sup> to overcome the issue of variability in primary cells of different origins. Then, we investigated whether CUG<sup>exp</sup> RNA induced cellular senescence and which senescence process was key in DM1 pathogenesis.

## MATERIALS AND METHODS

### Cell Culture and Transfection

Plasmid pLC16 was used for conditional transcription of expanded CTG repeats, as previously described (Nakamori et al., 2011b). Briefly, pLC16 consists of a cytomegalovirus/chicken  $\beta$ -actin enhancer/promoter, followed by a floxed selection-stop cassette, a downstream complementary DNA (cDNA) sequence for hygromycin resistance, and, finally, the human *DMPK* 3'-UTR, modified with restriction sites for insertion of expanded CTG repeats (**Supplementary Figure S1A**). The selection-stop cassette contains cDNA encoding a puromycin resistance protein (*puro*) followed by a triple-stop transcription terminator. The expanded CTG repeat was synthesized in the repeat donor plasmid pDWD using cell-free cloning by amplification of dimerized expanded repeats. The expanded CTG repeat was inserted into the *DMPK* 3'-UTR sequence in the pLC16 plasmid construct.

DM1 fibroblasts (GM05281) were purchased from Coriell Institute. DM1 myoblasts were obtained from biopsy

specimens as described previously (Nakamori et al., 2017). Human fetal lung fibroblasts (TIG-3 cells, passage 20) were obtained from the Japanese Collection of Research Bioresources Cell Bank. They were cultured in Dulbecco's modified Eagle medium with low glucose (Gibco) supplemented with 10% fetal bovine serum. Then, the TIG-3 cells were cotransfected with pLC16 containing 800 CTG repeats and phiC31 integrase using Nucleofector Technology with program U-023 (Lonza). Stably transfected cells were selected with puromycin (0.5  $\mu$ g/ml). The expression of expanded CUG RNA was induced by *Cre* recombinase-mediated excision of the *puro*-transcription-terminator cassette. Cells with recombination were selected using hygromycin B (50  $\mu$ g/ml). The proliferative capacity of the cells was assessed by calculating CPDL, as previously described (Bigot et al., 2009).

### Fluorescent *in situ* Hybridization (FISH)

FISH was performed as previously described (Nakamori et al., 2011b). The resultant fluorescence images were obtained using a BZ-X710 fluorescence microscope (Keyence).

### SA- $\beta$ -Gal and BrdU Activity and Proliferative Capacity

SA- $\beta$ -gal activity was determined using a Senescence Cells Histochemical Staining Kit (Sigma-Aldrich), according to the manufacturer's protocol. Images were obtained with a BZ-X710 fluorescence microscope. Proliferating cells were detected using a BrdU Immunohistochemistry Kit (Abcam), according to the manufacturer's protocol. Briefly, the cells were incubated with 10  $\mu$ M BrdU for 24 h at 37°C. BrdU-positive cells were analyzed using ImageJ software (National Institutes of Health).

### Quantitative RT-PCR

Total RNA was extracted from the DM1 model cells using an RNeasy Mini Kit (Qiagen). Then, the RNA was reverse transcribed to cDNA using a Superscript III First-Strand Synthesis System (Invitrogen), according to the manufacturer's protocol. qPCR was performed using TaqMan Gene Expression assays on an ABI PRISM 7900HT Sequence Detection System (Applied Biosystems). Gene expression was determined using TaqMan primers and probes for *CDKN1A*, *TP53*, *CDKN2A*, *IGFBP3*, *SERPINE1*, *NQO1*, *HMOX1*, *MMP1*, and *MMP3* (Applied Biosystems). Relative mRNA expression was normalized to 18S rRNA. The level of endogenous *DMPK* plus transgene-derived mRNA was determined as described previously (Nakamori et al., 2011a). Alternative splicing of *MBNL1* exon 5 and *MBNL2* exon 5 was analyzed as described previously (Nakamori et al., 2016).

### RNA-Seq Analysis

Whole transcriptome RNA-seq analysis was performed on CUG<sup>exp-</sup> and CUG<sup>exp+</sup> cells using a NovaSeq 6,000 System (Illumina). The raw data were evaluated by NGQC software (Novogene) and trimmed to remove adaptor contaminants and low-quality reads. Clean reads were aligned to the reference genome sequence using TopHat v2.0.12

(Trapnell et al., 2009). The estimated transcript abundance was calculated, and the count values were normalized to the upper quartile of the fragments per kilobase of transcript per million mapped reads using HTSeq v0.6.1 (Anders et al., 2015). GO enrichment analyses were conducted using goseq v2.12.0 (Young et al., 2010) and Metascape (<http://www.metascape.org>). Sequencing data have been deposited in Gene Expression Omnibus under accession number GSE196265.

## Western Blot

Total cell proteins were prepared from the DM1 model cells, as previously described (Nakamori et al., 2017). Then, the proteins were separated by sodium dodecyl sulfate-polyacrylamide gel electrophoresis and immunoblotted with the following primary antibodies: mouse anti-IGFBP3 (1:500; MAB305, R&D Systems), rabbit anti-PAI-1 (1:2000; NBP1-19773, Novus), rabbit anti-AKT (1:500; GTX121937, GeneTex), rabbit anti-phospho-Akt (Ser473) (1:500; 4,058, Cell Signaling Technology), rabbit anti-p53 (1:100; 2,527, Cell Signaling Technology), rabbit anti-p21 (1:1,000; 2,947, Cell Signaling Technology), rabbit anti-p16 (1:1,000; ab108349, Abcam), and rabbit anti-GAPDH (1:1,000; G9545, Sigma-Aldrich). After incubation, the immunoblots were washed, incubated with horseradish peroxidase-conjugated anti-mouse immunoglobulin (Ig) G or anti-rabbit IgG (GE Healthcare), and detected by ECL Prime Western Blotting Detection Reagent (GE Healthcare) using a ChemiDoc Touch Imaging System (Bio-Rad).

## Enzyme-Linked Immunosorbent Assay for Secreted IGFBP-3

The levels of secreted IGFBP-3 were measured using a Human IGFBP-3 Quantikine ELISA Kit (R&D Systems), according to the manufacturer's instructions. Recombinant human IGFBP-3 protein (R&D Systems) was used as the standard control.

## Telomere Length Measurement

Genomic DNA was extracted from the DM1 model cells using a Genra Puregene Cell Kit (Qiagen). Then, telomere length was measured using a Relative Human Telomere Length Quantification qPCR Assay Kit (ScienCell), according to the manufacturer's protocol. Briefly, the extracted genomic DNA was added to a reaction containing a primer pair (telomere or single copy reference) and Power SYBR Green PCR Master Mix (Applied Biosystems). PCR was performed on an ABI PRISM 7900HT Sequence Detection System (Applied Biosystems).

## Comet Assay

Comet assays were performed, as previously described (Olive and Banath, 2006). Briefly, cell suspensions were mixed with a 1% low-gelling-temperature agarose solution and spotted onto agarose-precoated glass slides. The slides were gently submerged in an alkaline lysis solution for 4 h at 4°C and then transferred to an electrophoresis solution and electrophoresed at 20 V for 25 min. Next, the slides were submerged in rinse buffer for 30 min at room temperature and then incubated with 2.5 µg/ml SYBR Green I Nucleic Acid Gel Stain (Invitrogen) for 20 min.

The results were analyzed using ImageJ software and scored as the percentage of tail DNA and Olive tail moment.

## Immunofluorescence

The DM1 model cells were plated on Lab-Tek II chamber slides (Thermo Fisher Scientific) and incubated for 24 h. After washing with PBS, the cells were fixed in 4% paraformaldehyde for 15 min and permeabilized with 0.3% Triton for 5 min. Then, cells were blocked with 5% BSA for 30 min and incubated with mouse anti-phospho-Histone H2A.X (Ser139) antibody (1:500; 05-636, Merck Millipore) overnight at 4°C. After washing with PBS, cells were incubated with goat-anti-mouse Alexa 488 secondary antibody (1:500) for 1 h. Cells were washed with PBS and mounted with Vectashield Hardset mounting medium with DAPI (Vector Laboratories). The fluorescence images were obtained using a BZ-X710 fluorescence microscope (Keyence).

## Abasic Site Measurement

The number of AP sites was assessed using a colorimetric DNA Damage Quantification Kit-AP Site Counting (Dojindo), according to the manufacturer's instructions. The results were measured on a Multiskan FC Microplate Photometer (Thermo Fisher Scientific).

## Flow Cytometry Analysis of ROS Production and Mitochondrial Membrane Potential

ROS production was determined by flow cytometry using MitoSOX Red Mitochondrial Superoxide Indicator (Invitrogen), and the mitochondrial membrane potential was measured by flow cytometry using Rhodamine 123 (Invitrogen). Briefly, the DM1 model cells were seeded at a density of 80% confluency on 12-well plates. Then, H<sub>2</sub>O<sub>2</sub> (200 µM) was added to induce ROS production, and the cells were incubated at 37°C for 1 h. After detaching the cells from the wells using trypsin, they were incubated with 5 µM MitoSOX or 10 µM Rhodamine 123 for 30 min at 37°C. Finally, the cells were analyzed on a BD FACSCanto II flow cytometer (BD Biosciences). The total cell population was defined according to the forward versus side scatter dot plot, and data for the live cells only were extracted for analysis. The median fluorescence intensity (MFI) of at least 10,000 cells was analyzed using FlowJo software (BD Biosciences). Unstained cells were used as a control.

## ATP Measurement

The levels of cellular ATP were quantified using an Intracellular ATP Assay Kit v2 (TOYO B-Net), according to the manufacturer's instructions. The emitted luciferin luminescence was quantified using a Glomax 20/20 Luminometer (Promega). Results were corrected for protein concentration using ATP-extracted samples.

## Statistical Analysis

Data were presented as the mean ± standard deviation (SD) from at least three independent biological replicates. Statistical

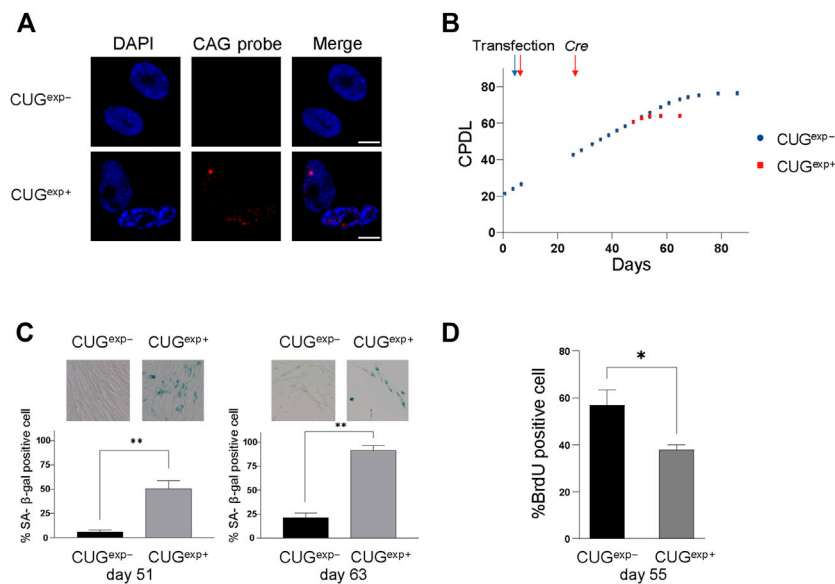


**FIGURE 1 |** Expanded CUG repeat RNA induces cellular senescence in DM1 model cells. **(A)** Representative images of RNA FISH analysis in cells not expressing CUG<sup>exp</sup> (CUG<sup>exp-/-</sup>) and cells expressing CUG<sup>exp</sup> (CUG<sup>exp+/+</sup>) at day 53. Nuclear CUG<sup>exp</sup> foci were present in CUG<sup>exp+/+</sup> cells. Scale bar: 10  $\mu$ m. DAPI: 4',6-diamidino-2-phenylindole. **(B)** Cumulative population doubling levels (CPDL) of CUG<sup>exp-/-</sup> cells (blue) and CUG<sup>exp+/+</sup> cells (red) during continuous passages. Cells were transfected with plasmid pLC16 containing 800 CTG repeats at day 6. CUG<sup>exp</sup> RNA was induced by Cre recombinase at day 25 in CUG<sup>exp-/-</sup> cells. Data are presented as means  $\pm$  SD of three independent experiments. **(C)** Senescence-associated  $\beta$ -galactosidase (SA- $\beta$ -gal) activity in CUG<sup>exp-/-</sup> and CUG<sup>exp+/+</sup> cells at day 51 (left) and day 63 (right). Representative images of SA- $\beta$ -gal staining (top). Bar graph shows the percentage of SA- $\beta$ -gal-positive cells (bottom). Data are presented as means  $\pm$  SD of three independent experiments. \*\* $p < 0.001$ . **(D)** Immunohistochemical quantification of the percentage of BrdU-positive cells at day 55. Data are presented as means  $\pm$  SD of three independent experiments. \* $p < 0.01$ .

significance was tested using the Student's *t*-test. *p* values <0.05 were considered statistically significant.

## RESULTS

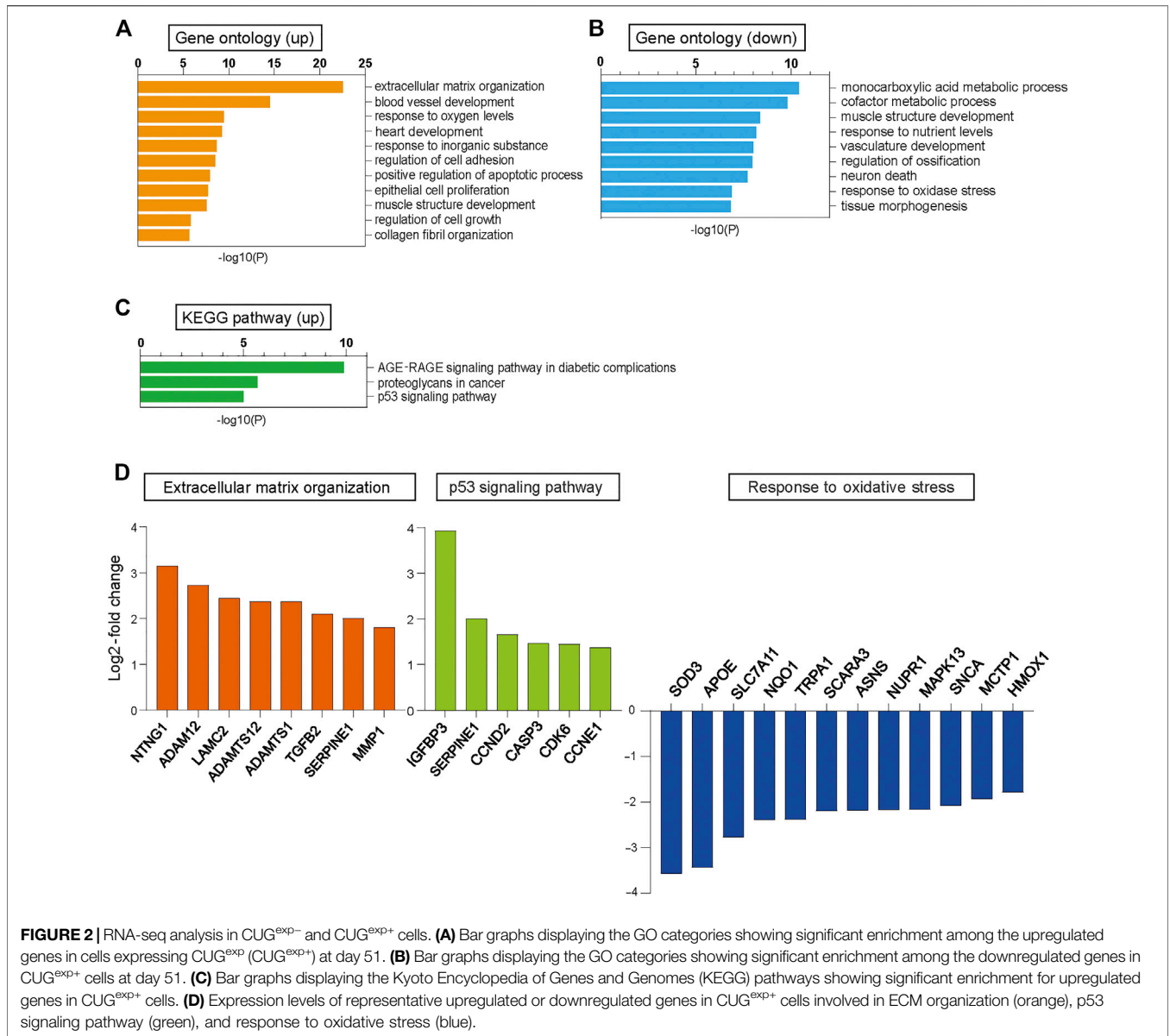
### Expanded CUG Repeat RNA Induces Cellular Senescence in DM1 Model Cells

We developed a DM1 cell model to investigate the effect of CUG<sup>exp</sup> RNA on cellular senescence. First, we transfected normal human lung fibroblasts (TIG-3 cells) with plasmid pLC16 containing 800 CTG repeats (day 6). Then, we treated the cells with Cre recombinase, and obtained DM1 model cells conditionally expressing CUG<sup>exp</sup> RNA after 18 days of selection using hygromycin B (day 47). This cell model allowed us to control CUG<sup>exp</sup> RNA expression in primary cells with the same genetic background so that we could assess the mechanism of cellular senescence by CUG<sup>exp</sup> RNA expression more accurately than in patient-derived cells.

In the cells expressing CUG<sup>exp</sup> RNA following induction by Cre recombinase, the total expression level of transgene and endogenous *DMPK* was increased 3.8-fold compared with that of endogenous *DMPK* and DM1 fibroblasts and to a similar level in DM1 myoblasts (**Supplementary Figure S1B**). RNA-fluorescence *in situ* hybridization (FISH) experiments showed RNA foci formation, as observed in DM1 patient cells (**Figure 1A**; **Supplementary Figure S1C**). Splicing misregulation in *MBNL1* and *MBNL2* was also induced by CUG<sup>exp</sup> RNA expression

(**Supplementary Figure S1D**). We calculated the cumulative population doubling level (CPDL) by culturing the DM1 model cells to compare the proliferative capacity of cells expressing CUG<sup>exp</sup> (CUG<sup>exp+/+</sup> cells) with those not expressing CUG<sup>exp</sup> (CUG<sup>exp-/-</sup> cells). The induction of abnormal RNA slowed cell proliferation and prematurely terminated cell division (**Figure 1B**; **Supplementary Figure S2A**). We also confirmed that the induction of CUG<sup>exp</sup> RNA reduced the proliferative capacity in two other independently established TIG-3 cell lines conditionally expressing CUG<sup>exp</sup> RNA (**Supplementary Figure S2B**). However, the integration sites of the transgene and the expression level of CUG<sup>exp</sup> RNAs are different in each cell line. Therefore, to avoid the effect of variation in genetic background, we further investigated the mechanism of the premature arrest of cell proliferation in a representative cell line with a sufficient evaluation period after the induction of CUG<sup>exp</sup> RNA expression in the same genetic background. Furthermore, we confirmed that Cre induction and hygromycin B selection did not affect cell proliferation in TIG-3 cells transfected with plasmid pLC16 containing no CTG repeat (**Supplementary Figure S2C**).

We examined the activity of senescence-associated  $\beta$ -galactosidase (SA- $\beta$ -gal), a biomarker of senescent cells, to clarify whether the premature arrest was associated with senescence. There were 9.4-fold and 4.3-fold increases in SA- $\beta$ -gal positivity in CUG<sup>exp+/+</sup> cells compared with CUG<sup>exp-/-</sup> cells on day 51 and day 63, respectively ( $p = 0.0008$  and  $0.00006$ , respectively, **Figure 1C**). Furthermore, CUG<sup>exp+/+</sup> cells showed significantly lower levels of bromodeoxyuridine (BrdU) positivity



(indicating cells with proliferative activity) compared with CUG<sup>exp-</sup> cells ( $p = 0.0083$ , **Figure 1D**). Thus, CUG<sup>exp</sup> expression induced early arrest of cell division and senescence in the DM1 model cells.

### Expanded CUG Repeat RNA Alters Gene Expression Profiles Related to Cellular Senescence

We performed RNA sequencing (RNA-seq) analysis in CUG<sup>exp+</sup> and CUG<sup>exp-</sup> cells at day 51 to identify the pathway that induced cellular senescence when CUG<sup>exp</sup> RNA was expressed. Up-regulated and down-regulated genes in CUG<sup>exp+</sup> cells had some overlap with those in DM1 myoblasts or myotubes reported in a previous study, despite the cell type difference (Todorow et al., 2021) (**Supplementary Table S1**). Gene ontology

(GO) enrichment analysis was performed to identify relevant biological pathways. Genes for extracellular matrix (ECM) organization, positive regulation of the apoptotic process, and regulation of cell growth were highly enriched among the upregulated genes in CUG<sup>exp+</sup> cells (**Figure 2A**). The genes involved in ECM organization included *MMP1* and *ADAMT* genes (**Figure 2D**). These genes encode ECM-degrading enzymes, which are important molecules comprising the SASP (Mavrogonatou et al., 2019). Among the ECM-degrading enzymes, the matrix metalloproteinase (MMP) family is predominantly linked with cellular senescence (Mavrogonatou et al., 2019). For example, *MMP1* and *MMP3* expression was reported as upregulated in senescent fibroblasts (Coppe et al., 2010). We evaluated *MMP1* and *MMP3* expression in the DM1 model cells at days 51 and 63 by quantitative reverse transcription-polymerase chain reaction (qRT-PCR) and found

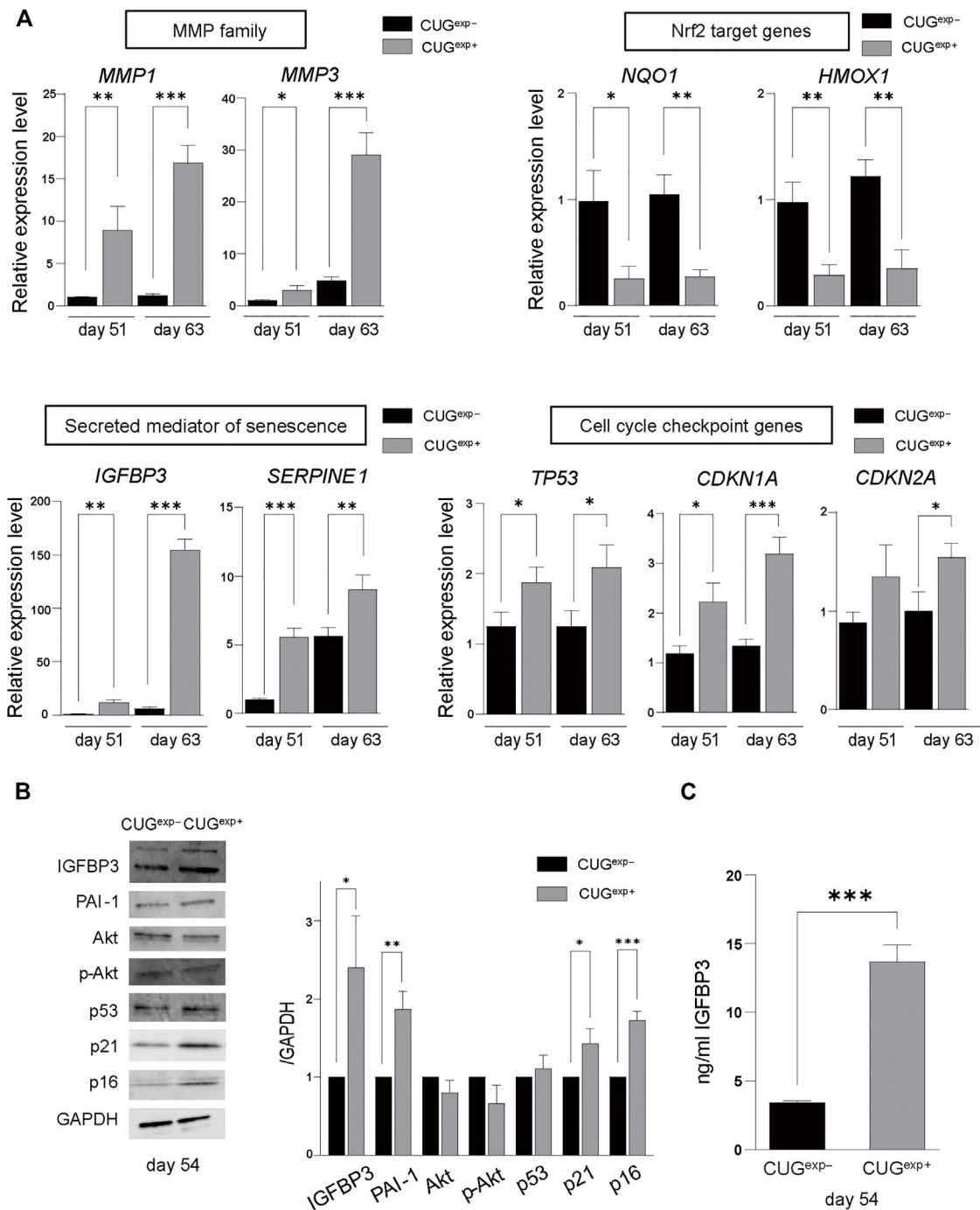


**FIGURE 3 |** Expanded CUG repeat RNA alters gene and protein expression levels related to cellular senescence. **(A)** Gene expression levels of MMP family genes (*MMP1* and *MMP3*) (top left), Nrf2 target genes (*NQO1* and *HMOX1*) (top right), secreted mediators of senescence (*IGFBP3* and *SERPINE1*) (bottom left), and cell cycle checkpoint genes (*TP53*, *CDKN1A*, and *CDKN2A*) (bottom right) determined by qRT-PCR in cells not expressing CUG<sup>exp</sup> (CUG<sup>exp-</sup>) and cells expressing CUG<sup>exp</sup> (CUG<sup>exp+</sup>) cells at days 51 and 63. Values are presented as means ± SD of three independent experiments. \**p* < 0.05, \*\**p* < 0.01, and \*\*\**p* < 0.001. **(B)** Representative images of western blots of IGFBP3, PAI-1, Akt, phospho-Akt (Ser437), p53, p21, and p16 proteins in CUG<sup>exp-</sup> and CUG<sup>exp+</sup> cells at day 54 (left). GAPDH was used as the loading control. Bar graph shows quantification of the immunoblot (right). Values are presented as means ± SD of three independent experiments. \**p* < 0.05, \*\**p* < 0.01, and \*\*\**p* < 0.001. **(C)** IGFBP3 levels in the culture medium of CUG<sup>exp-</sup> and CUG<sup>exp+</sup> cells at day 54. Values are presented as means ± SD of three independent experiments. \*\*\**p* < 0.001.

that the expression of these genes was significantly increased in CUG<sup>exp+</sup> cells ( $p = 0.0087$  and  $0.023$  at day 51, and  $p = 0.0002$  and  $0.0007$  at day 63, respectively, **Figure 3A**), suggesting that CUG<sup>exp</sup> RNA alters the expression of several ECM-degrading enzymes related to cellular senescence. Genes for muscle structure development and response to oxidative stress were significantly enriched among the downregulated genes (**Figure 2B**). The genes involved in the response to oxidative stress and antioxidant expression, such as *NQO1* and *HMOX1*, were significantly decreased ( $p = 0.016$  and  $0.005$  at day 51, and  $p = 0.0026$  and  $0.0031$  at day 63, respectively, **Figures 2D, 3A**).

Furthermore, Kyoto Encyclopedia of Genes and Genomes (KEGG) pathway analysis showed that the p53 signaling pathway was highly enriched among the upregulated genes in CUG<sup>exp+</sup> cells (**Figure 2C**). This pathway involves *SERPINE1*, encoding plasminogen activator inhibitor-1 (PAI-1), and *IGFBP3*, a downstream target of PAI-1-induced senescence, which were both markedly upregulated ( $p = 0.0003$  and  $0.0014$  at day 51, and  $p = 0.0095$  and  $0.00002$  at day 63, respectively, **Figures 2D, 3A**). These genes were reported not only as markers of senescence but also as inducers of senescence in human and mouse fibroblasts (Debacq-Chainiaux et al., 2008; Vaughan et al., 2017). The protein levels of PAI-1 and insulin-like growth factor binding protein 3 (IGFBP3) were also significantly increased in CUG<sup>exp+</sup> cells at day 54 ( $p = 0.0026$  and  $0.021$ , respectively, **Figure 3B**). We then assessed the activity of Akt, a critical downstream target downregulated by PAI-1 and IGFBP3 (Balsara et al., 2006; Elzi et al., 2012). Akt phosphorylation at Ser473 was mildly decreased in CUG<sup>exp+</sup> cells at day 54, although this was not statistically significant ( $p = 0.065$ , **Figure 3B**). IGFBP3 has also been reported as a secreted mediator of cellular senescence with paracrine and autocrine activity (Vassilieva et al., 2020). The IGFBP3 levels in the culture medium of the DM1 model cells showed a 4-fold increase in CUG<sup>exp+</sup> cell cultures at day 54 ( $p = 0.00013$ , **Figure 3C**). These results indicated that the PAI-1-IGFBP3 pathway was activated by CUG<sup>exp</sup> RNA expression in the DM1 model cells.

## Expanded CUG Repeat RNA Activates Cell Cycle Checkpoint Inhibitors

PAI-1 and IGFBP3 were reported as induced by p53 activation (Grimberg et al., 2005; Vaughan et al., 2017). p53 is activated in response to DNA damage and various stressors that characteristically promote cellular senescence to regulate the cell cycle (Di Micco et al., 2021). Cell cycle checkpoint genes, such as *TP53* encoding p53, *CDKN1A* encoding p21, and *CDKN2A* encoding p16, induce cellular senescence despite the presence of metabolic activity (Hernandez-Segura et al., 2018; McHugh and Gil, 2018). To investigate the influence of CUG<sup>exp</sup> RNA on cell cycle arrest, we measured the expression levels of cell cycle-related genes by qRT-PCR in CUG<sup>exp-</sup> and CUG<sup>exp+</sup> cells at days 51 and 63. *TP53* and *CDKN1A* were significantly increased in CUG<sup>exp+</sup> cells ( $p = 0.021$  and  $0.011$  at day 51, and  $p = 0.021$  and  $0.0009$  at day 63, respectively, **Figure 3A**). *CDKN2A* was mildly increased in CUG<sup>exp+</sup> cells at day 51 ( $p = 0.076$ , **Figure 3A**) and significantly increased at day 63 ( $p = 0.017$ , **Figure 3A**). The

protein levels of p21 and p16 were significantly increased in CUG<sup>exp+</sup> cells at day 54 ( $p = 0.018$  and  $0.00043$ , respectively, **Figure 3B**). p53 was also mildly increased in CUG<sup>exp+</sup> cells, although the increase did not reach statistical significance ( $p = 0.33$ , **Figure 3B**). p21 and p16 are sufficient to establish cell cycle arrest in an independent and interdependent manner (McHugh and Gil, 2018; Di Micco et al., 2021). Our results indicated that CUG<sup>exp</sup> RNA expression increased the expression of cell cycle checkpoint inhibitors, resulting in cell cycle arrest in the DM1 model cells.

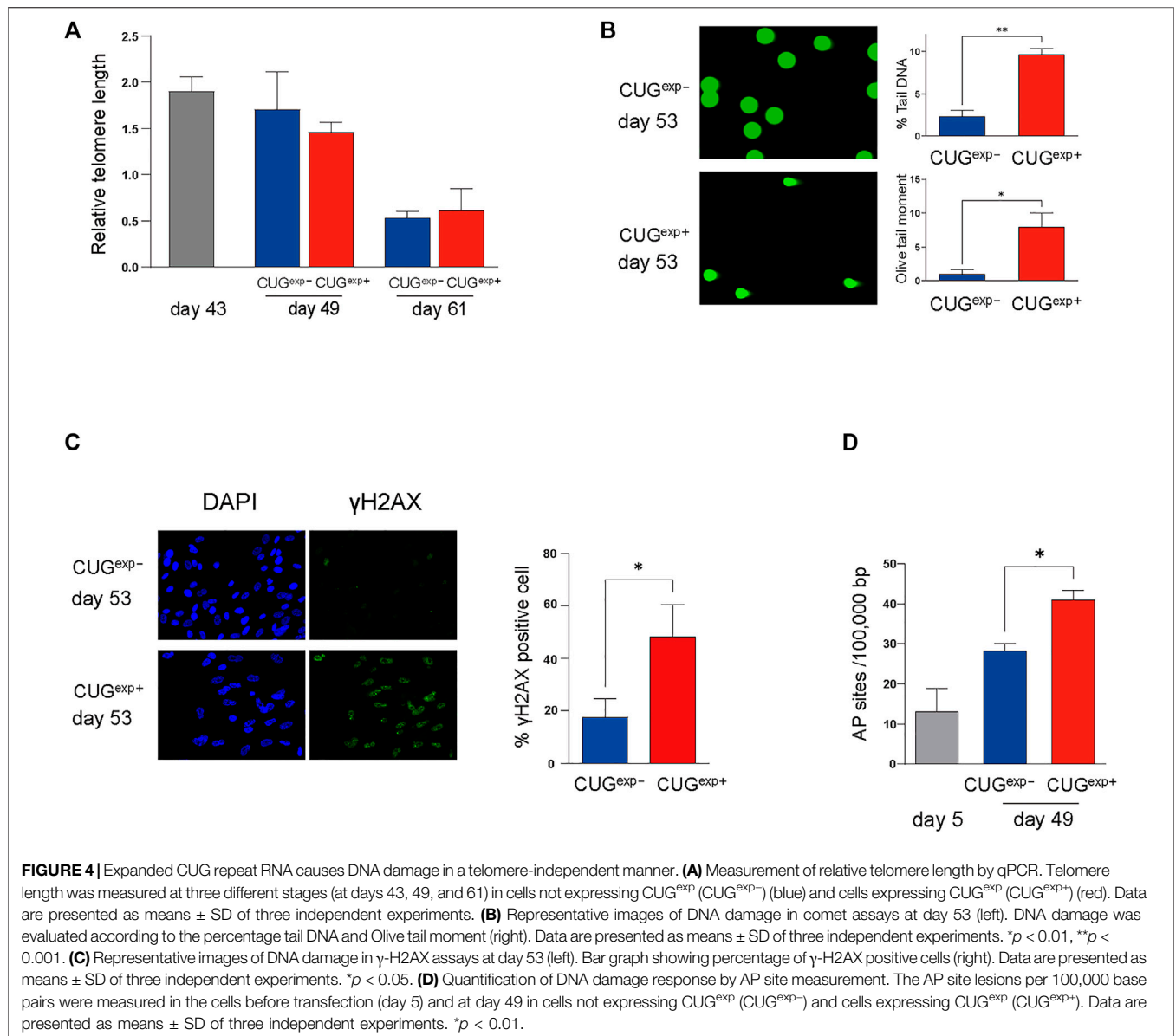
## Expanded CUG Repeat RNA Causes DNA Damage in a Telomere-Independent Manner

Next, we investigated the regulatory mechanism responsible for the increased levels of cell cycle inhibitors p21 and p16 and secreted mediators IGFBP3 and PAI-1 in the DM1 model cells. Telomere shortening is an important molecular mechanism of cell cycle arrest (Di Micco et al., 2021). Shortened telomeres are recognized as DNA breaks, and they promote cell cycle arrest, known as replicative senescence (Hernandez-Segura et al., 2018; Di Micco et al., 2021). We used qPCR to measure the telomere length in the DM1 model cells at days 43, 49, and 61 to confirm whether the cellular senescence induced by CUG<sup>exp</sup> occurred in a telomere-dependent manner. Although the telomere length in CUG<sup>exp-</sup> and CUG<sup>exp+</sup> cells was shortened in later passages, there was no significant difference in the telomere length between both cell types (**Figure 4A**). This suggested that telomere shortening was not associated with accelerated cellular senescence caused by the toxic CUG<sup>exp</sup> RNA.

Telomere-independent senescence (premature senescence) occurs when DNA damage response (DDR) is triggered in response to DNA damage, even in normal proliferating cells (Di Micco et al., 2021). We performed a comet assay on the DM1 model cells to evaluate the DNA damage induced by CUG<sup>exp</sup>. The parameters reflecting the extent of DNA damage, such as the percentage tail DNA and Olive tail moment (OTM), were significantly increased in CUG<sup>exp+</sup> cells at day 53 ( $p = 0.00022$  and  $0.0056$ , respectively, **Figure 4B**). Furthermore,  $\gamma$ -H2AX foci, indicative of DNA damage, were significantly increased in CUG<sup>exp+</sup> cells ( $p = 0.019$ , **Figure 4C**). Next, we evaluated apurinic/apyrimidinic (AP) sites (markers of base excision repair) to confirm DDR activation in response to DNA damage in the DM1 model cells. The AP site lesions were increased in later passages and were more significantly increased in CUG<sup>exp+</sup> cells at day 49 ( $p = 0.0015$ , **Figure 4D**), suggesting that abnormal CUG<sup>exp</sup> RNA increased DNA damage and DDR in the DM1 model cells.

## Expanded CUG Repeat RNA Impairs Mitochondrial Function and Increases Reactive Oxygen Species

We then investigated the cause of DNA damage in CUG<sup>exp+</sup> cells. ROS are important in the induction of cellular senescence because they damage DNA *via* a variety of mechanisms, including



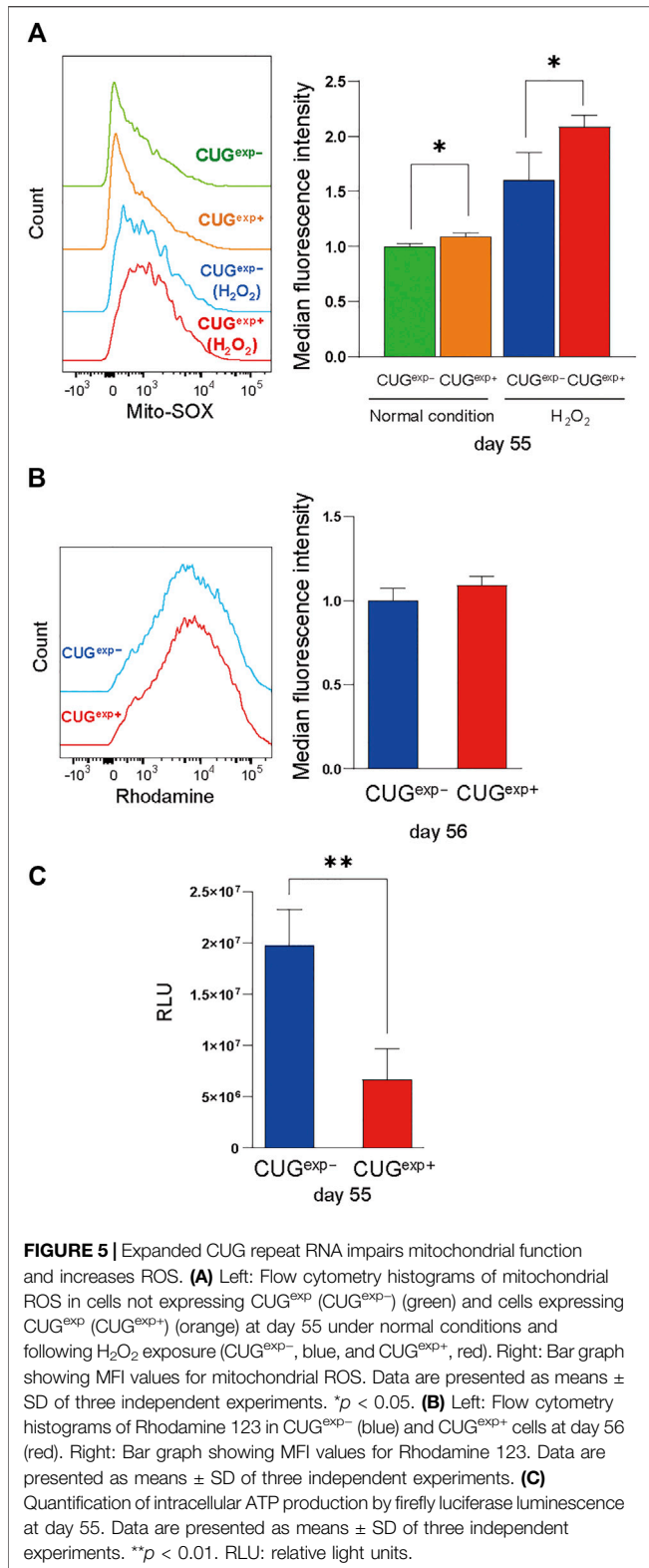
oxidized DNA bases, AP sites, and double-strand breaks (Davalli et al., 2016). Considering the possibility that excessive ROS production may cause the DNA damage by toxic repeat RNA, we measured mitochondrial ROS by flow cytometry. H<sub>2</sub>O<sub>2</sub>, which induces intracellular ROS generation, was added to evaluate the response to oxidative stress (Weng et al., 2018). In our study, mitochondrial ROS were significantly increased in CUG<sup>expD+</sup> cells at day 55 under normal conditions, and the difference was more pronounced following H<sub>2</sub>O<sub>2</sub> exposure (*p* = 0.018 and 0.036, respectively, **Figure 5A**).

Mitochondria are the major sites of ROS production (Turrens, 2003) and mitochondrial dysfunction contributes to ROS overproduction (Korolchuk et al., 2017). Therefore, we evaluated mitochondrial dysfunction as a cause of ROS production. Rhodamine 123, which accumulates in activated mitochondria that have a high membrane potential, was

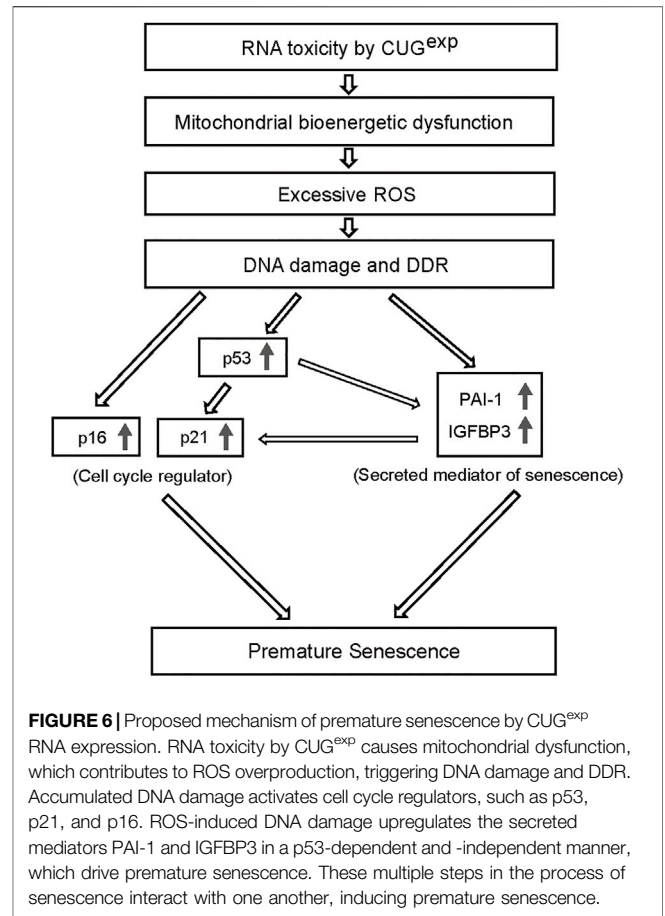
unaffected by CUG<sup>expD</sup> RNA expression (**Figure 5B**). However, although the mitochondrial membrane potential remained unchanged, intracellular ATP levels were significantly decreased in CUG<sup>expD+</sup> cells at day 55 (*p* = 0.0082, **Figure 5C**). Decreased cellular ATP production results from mitochondrial bioenergetic dysfunction, and insufficient mitochondrial energy production leads to excessive ROS production (Korolchuk et al., 2017). Thus, our results indicated that CUG<sup>expD</sup> RNA caused mitochondrial dysfunction, contributing to premature senescence *via* ROS production.

## DISCUSSION

The presentation of multisystemic symptoms that resemble features of aging in patients with DM1, such as muscle



wasting, cataract, cognitive impairment, and frontal baldness, suggests DM1 as a progeroid disorder (Meinke et al., 2018). Although several studies of DM1 patient-derived cells indicate



the involvement of cellular senescence (Furling et al., 2001; Bigot et al., 2009; Thornell et al., 2009; Renna et al., 2014), the senescence process remains unelucidated. In this study, we established a primary cell model of DM1 with the conditional expression of CUG<sup>exp</sup> RNA. We demonstrated that CUG<sup>exp</sup> expression induced premature senescence in the DM1 model cells. Additionally, our results suggest that premature senescence in the DM1 model cells is associated with mitochondrial dysfunction and ROS production, leading to the upregulation of secreted mediators IGFBP3 and PAI-1 and cell cycle regulators p16, p21, and possibly p53 (Figure 6).

Cellular senescence is defined as the permanent cessation of cell proliferation. It is induced by two distinct mechanisms: replicative senescence (triggered by telomere loss) and premature senescence (caused by a telomere-independent mechanism) (Kuilman et al., 2010). Our results suggest that the expression of CUG<sup>exp</sup> RNA induces cellular senescence regardless of telomere length, which correlates with the findings of another study reporting reduced proliferative capacity in muscle satellite cells from patients with DM1, even though the telomeres did not reach a critical size (Bigot et al., 2009).

Telomere-independent premature senescence is triggered by various cellular stressors, including oxidative stress, oncogene activation, and DNA damage agents such as ionizing radiation or

chemotherapeutic substances (Kuilman et al., 2010; Hernandez-Segura et al., 2018). Exposure to these stressors induces persistent DNA damage and DDR, resulting in premature senescence. Our study focused on oxidative stress, a typical internal factor that causes premature senescence, because the use of our DM1 cell model allowed us to exclude the influence of external factors. Oxidative stress is characterized by ROS overproduction (Davalli et al., 2016). ROS directly damage DNA, causing the induction and maintenance of cellular senescence (Passos et al., 2010; Davalli et al., 2016). The majority of ROS are produced in mitochondria, and mitochondrial ROS production increases with mitochondrial metabolic dysfunction (Turrens, 2003; Korolchuk et al., 2017). Mitochondrial ROS were slightly but significantly increased in CUG<sup>exp+</sup> cells solely by induction of abnormal RNA expression even in physiological condition. Previous studies demonstrated that even slight changes in mitochondrial ROS production are associated with DNA damage and mitochondrial dysfunction in fibroblasts (Kobashigawa et al., 2015; Lofaro et al., 2020). Our findings of increased mitochondrial ROS, decreased intracellular ATP, and DDR activation in CUG<sup>exp+</sup> cells indicate that CUG<sup>exp</sup> RNA promotes ROS-mediated premature senescence by mitochondrial dysfunction.

ROS homeostasis is maintained by antioxidants. Nuclear factor-erythroid 2 related factor 2 (Nrf2) transcriptionally regulates several antioxidant genes, such as *HMOX1* and *NQO1*, to decrease ROS levels (Kasai et al., 2020). On the other hand, excess ROS activates p53, which suppresses the Nrf2-regulated antioxidant genes (Drane et al., 2001; Faraonio et al., 2006). Nrf2-dependent antioxidant factors were decreased in our CUG<sup>exp+</sup> DM1 model cells, suggesting that Nrf2, which is normally activated to eliminate excessive ROS, is suppressed by p53, exacerbating the vulnerability of our DM1 model cells to oxidative stress. Moreover, oxidative stress has been clinically associated with cataracts (Pendergrass et al., 2005), frontal hair loss (Shin et al., 2013), and metabolic dysfunction (de Almeida et al., 2017), which are commonly observed in patients with DM1. Furthermore, antioxidant capacity has been reported as impaired in DM1 patients' serum (Toscano et al., 2005; Kumar et al., 2014). These findings suggest that ROS-induced premature senescence leads to the features of aging observed in DM1.

The mechanism of cell cycle arrest by CUG<sup>exp</sup> RNA is largely unknown. The cell cycle is chiefly regulated by the p53-p21 and p16-pRb pathways. Although these pathways have complex interactions, p16 is mainly involved in maintaining cellular senescence by mitogenic stress and sustained DDR (Mijit et al., 2020; Di Micco et al., 2021). Muscle satellite cells derived from patients with congenital DM1 have been reported to induce p16-dependent premature senescence (Bigot et al., 2009). In our study, p16 and p21 expression was significantly increased in CUG<sup>exp+</sup> cells at both the transcript and protein levels. Moreover, p53 expression was significantly increased in CUG<sup>exp+</sup> cells at the transcript level and mildly increased at the protein level. The p53-p21 pathway, which is necessary for senescence induction, is upregulated following DDR activation (Mijit et al., 2020; Di Micco et al., 2021). Thus, our data indicate that abnormal CUG<sup>exp</sup> RNA can

induce senescence by activating the p53-p21 pathway and cause irreversible senescence by p16 upregulation.

PAI-1 and IGFBP3 are major factors affecting cellular senescence, mainly as downstream targets of p53 (Grimberg et al., 2005; Vaughan et al., 2017; Vassilieva et al., 2020). In our study, the transcript and protein levels of PAI-1 and IGFBP3 were significantly increased in CUG<sup>exp+</sup> cells. PAI-1 and IGFBP3 are regulated in both p53-dependent and -independent manner in response to ROS-induced DNA damage (Grimberg et al., 2005; Eren et al., 2014). Hence, CUG<sup>exp</sup> RNA may increase the expression of PAI-1 and IGFBP3 not only through p53 but also through another signaling pathway activated by ROS-induced DNA damage. Further, PAI-1 and IGFBP3 induce cellular senescence with activation of cell cycle inhibitors. For example, IGFBP3 overexpression upregulates p21 in some cancer cells (Wu et al., 2013), and inhibition of PAI-1 activity reduces p16 expression (Eren et al., 2014). Therefore, the excessive ROS, DNA damage, and DDR observed in CUG<sup>exp+</sup> cells may increase PAI-1 and IGFBP3, leading to premature senescence *via* activation of cell cycle inhibitors. Additionally, Akt is involved in PAI-1- and IGFBP3-induced cell growth suppression and cellular senescence (Balsara et al., 2006; Elzi et al., 2012). We observed a slight reduction in Akt activity in CUG<sup>exp+</sup> cells, which is consistent with a previous study using fibroblasts from DM1 patients (Garcia-Puga et al., 2020). Our results suggest the possibility that abnormal CUG<sup>exp</sup> RNA can inactivate Akt, causing PAI-1- and IGFBP3-mediated senescence. Furthermore, recent studies have shown the suppression of Akt signaling in DM1 skeletal muscle, so reduced Akt activity may be associated with skeletal muscle atrophy (Crawford Parks et al., 2017; Sabater-Arcis et al., 2020; Ozimski et al., 2021). Skeletal muscle atrophy is generally associated with mitochondrial ROS (Powers, 2014), and PAI-1 inhibits the regeneration of damaged skeletal muscle (Rahman and Krause, 2020). Thus, the mechanism of cell proliferation inhibition via PAI-1 and IGFBP3 by ROS-induced DNA damage may also contribute to muscle atrophy in DM1. However, it should be noted that the mechanism of premature senescence observed in our DM1 model fibroblast cells could be different in DM1 myoblast cells. Even in myoblasts, a different mechanism of premature senescence was reported in DM1 and DM2 (Renna et al., 2014).

Previous studies have suggested that cellular senescence in DM1 is associated with mitochondrial dysfunction, oxidative stress, DNA damage, and activation of cell cycle inhibitors (Hasuike et al., 2022). Our study demonstrated the direct effects of abnormal CUG<sup>exp</sup> RNAs on these factors by using the DM1 model cells conditionally expressing CUG<sup>exp</sup>. However, we were unable to evaluate either the characteristics of CUG<sup>exp+</sup> cells at a pre-senescence stage or the therapeutic effect by targeting CUG<sup>exp</sup> RNA or ROS, since CUG<sup>exp+</sup> cells exhibited delayed cell proliferation soon after the cell model establishment (day 47). Hence, it is not clearly determined whether the senescence inducers such as mitochondrial dysfunction and ROS production observed in CUG<sup>exp+</sup> cells are the cause or result of premature senescence. Generally, senescence occurs in a bidirectional manner and via various positive feedback

mechanisms. For example, cell cycle regulators, such as p53, p21, and p16, produce ROS as a downstream signal transduction factor without oxidative DNA damage, while ROS itself induces p53 (Davalli et al., 2016). Furthermore, the positive feedback loops of mitochondrial damage, ROS production, and DDR activation via the p53-p21 pathway are necessary and sufficient to maintain cell cycle arrest (Passos et al., 2010). Our data suggest that the activation of these positive feedback loops maintains senescence in CUG<sup>exp+</sup> cells. Several studies have shown impaired mitochondrial function in DM1 (Gramegna et al., 2018; Garcia-Puga et al., 2020). Thus, excessive ROS production by mitochondrial metabolic dysfunction may trigger the series of senescence pathways induced by CUG<sup>exp</sup> RNA.

In conclusion, our findings indicate that abnormal expanded CUG repeat RNA leads to mitochondrial dysfunction, ROS production, and DDR activation, and induces premature senescence. Various drug targets have been investigated to eliminate the influence of senescent cells and SASP (Di Micco et al., 2021). Interventions targeting the senescence-inducing factors resulting from CUG<sup>exp</sup> RNA may be potential therapeutics for symptoms that resemble accelerated aging in DM1.

## DATA AVAILABILITY STATEMENT

The datasets presented in this study can be found in online repositories. The names of the repository/repositories and accession number(s) can be found below: <https://www.ncbi.nlm.nih.gov/>, accession ID: GSE196265.

## REFERENCES

- Almeida, A. J. P. O. d., Ribeiro, T. P., and Medeiros, I. A. d. (2017). Aging: Molecular Pathways and Implications on the Cardiovascular System. *Oxidative Med. Cell Longevity* 2017, 1–19. doi:10.1155/2017/7941563
- Anders, S., Pyl, P. T., and Huber, W. (2015). HTSeq—a Python Framework to Work with High-Throughput Sequencing Data. *Bioinformatics* 31 (2), 166–169. doi:10.1093/bioinformatics/btu638
- Balsara, R. D., Castellino, F. J., and Ploplis, V. A. (2006). A Novel Function of Plasminogen Activator Inhibitor-1 in Modulation of the AKT Pathway in Wild-type and Plasminogen Activator Inhibitor-1-Deficient Endothelial Cells. *J. Biol. Chem.* 281 (32), 22527–22536. doi:10.1074/jbc.M512819200
- Bigot, A., Klein, A. F., Gasnier, E., Jacquemin, V., Ravassard, P., Butler-Browne, G., et al. (2009). Large CTG Repeats Trigger P16-dependent Premature Senescence in Myotonic Dystrophy Type 1 Muscle Precursor Cells. *Am. J. Pathol.* 174 (4), 1435–1442. doi:10.2353/ajpath.2009.080560
- Brook, J. D., McCurrach, M. E., Harley, H. G., Buckler, A. J., Church, D., Aburatani, H., et al. (1992). Molecular Basis of Myotonic Dystrophy: Expansion of a Trinucleotide (CTG) Repeat at the 3' End of a Transcript Encoding a Protein Kinase Family Member. *Cell* 68 (4), 799–808. doi:10.1016/0092-8674(92)90154-5
- Chang, H. Y., Chi, J.-T., Dudoit, S., Bondre, C., van de Rijn, M., Botstein, D., et al. (2002). Diversity, Topographic Differentiation, and Positional Memory in Human Fibroblasts. *Proc. Natl. Acad. Sci. U.S.A.* 99 (20), 12877–12882. doi:10.1073/pnas.162488599
- Charlet-B., N., Savkur, R. S., Singh, G., Philips, A. V., Grice, E. A., and Cooper, T. A. (2002). Loss of the Muscle-specific Chloride Channel in Type 1 Myotonic Dystrophy Due to Misregulated Alternative Splicing. *Mol. Cell* 10 (1), 45–53. doi:10.1016/s1097-2765(02)00572-5

## AUTHOR CONTRIBUTIONS

MN designed the research. MN and YH performed the research, analyzed the data, and wrote the manuscript. HM supervised the research. All authors contributed to the article and approved the submitted version.

## FUNDING

This work was supported by the Grant-in-Aid for Young Scientists and Grant-in-Aid for Scientific Research (B) (JSPS KAKENHI Grant Number JP 19K17007 and 21H02839), AMED (21ek0109438), and Intramural Research Grant for Neurological and Psychiatric Disorders of NCNP (2–5).

## ACKNOWLEDGMENTS

The authors thank Charles Thornton for his fundamental insight to conceptualize the study and Maiko Miyai for her technical assistance.

## SUPPLEMENTARY MATERIAL

The Supplementary Material for this article can be found online at: <https://www.frontiersin.org/articles/10.3389/fgene.2022.865811/full#supplementary-material>

- Coppé, J.-P., Patil, C. K., Rodier, F., Krtolica, A., Beauséjour, C. M., Parrinello, S., et al. (2010). A Human-like Senescence-Associated Secretory Phenotype Is Conserved in Mouse Cells Dependent on Physiological Oxygen. *PLoS One* 5 (2), e9188. doi:10.1371/journal.pone.0009188
- Crawford Parks, T. E., Ravel-Chapuis, A., Bondy-Chorney, E., Renaud, J.-M., Côté, J., and Jasmin, B. J. (2017). Muscle-specific Expression of the RNA-Binding Protein Staufin1 Induces Progressive Skeletal Muscle Atrophy via Regulation of Phosphatase Tensin Homolog. *Hum. Mol. Genet.* 26 (10), 1821–1838. doi:10.1093/hmg/ddx085
- Davalli, P., Mitic, T., Caporali, A., Lauriola, A., and D'Arca, D. (2016). ROS, Cell Senescence, and Novel Molecular Mechanisms in Aging and Age-Related Diseases. *Oxidative Med. Cell Longevity* 2016, 1–18. doi:10.1155/2016/3565127
- Debaq-Chainiaux, F., Pascal, T., Boilan, E., Bastin, C., Bauwens, E., and Toussaint, O. (2008). Screening of Senescence-Associated Genes with Specific DNA Array Reveals the Role of IGFBP-3 in Premature Senescence of Human Diploid Fibroblasts. *Free Radic. Biol. Med.* 44 (10), 1817–1832. doi:10.1016/j.freeradbiomed.2008.02.001
- Di Micco, R., Krizhanovsky, V., Baker, D., and d'Adda di Fagagna, F. (2021). Cellular Senescence in Ageing: from Mechanisms to Therapeutic Opportunities. *Nat. Rev. Mol. Cell Biol.* 22 (2), 75–95. doi:10.1038/s41580-020-00314-w
- Dolivo, D., Hernandez, S., and Dominko, T. (2016). Cellular Lifespan and Senescence: a Complex Balance between Multiple Cellular Pathways. *Bioessays* 38 (Suppl. 1), S33–S44. doi:10.1002/bies.201670906
- Drane, P., Bravard, A., Bouvard, V., and May, E. (2001). Reciprocal Down-Regulation of P53 and SOD2 Gene Expression—Implication in P53 Mediated Apoptosis. *Oncogene* 20 (4), 430–439. doi:10.1038/sj.onc.1204101
- Elzi, D. J., Lai, Y., Song, M., Hakala, K., Weintraub, S. T., and Shiio, Y. (2012). Plasminogen Activator Inhibitor 1 - Insulin-like Growth Factor Binding

- Protein 3 cascade Regulates Stress-Induced Senescence. *Proc. Natl. Acad. Sci. U.S.A.* 109 (30), 12052–12057. doi:10.1073/pnas.1120437109
- Eren, M., Boe, A., Klyachko, E., and Vaughan, D. (2014). Role of Plasminogen Activator Inhibitor-1 in Senescence and Aging. *Semin. Thromb. Hemost.* 40 (6), 645–651. doi:10.1055/s-0034-1387883
- Faraonio, R., Vergara, P., Di Marzo, D., Pierantoni, M. G., Napolitano, M., Russo, T., et al. (2006). p53 Suppresses the Nrf2-dependent Transcription of Antioxidant Response Genes. *J. Biol. Chem.* 281 (52), 39776–39784. doi:10.1074/jbc.M605707200
- Freyermuth, F., Rau, F., Kokunai, Y., Linke, T., Sellier, C., Nakamori, M., et al. (2016). Splicing Misregulation of SCN5A Contributes to Cardiac-Conduction Delay and Heart Arrhythmia in Myotonic Dystrophy. *Nat. Commun.* 7, 11067. doi:10.1038/ncomms11067
- Fu, Y. H., Pizzutti, A., Fenwick, R. G., Jr., King, J., Rajnarayan, S., Dunne, P. W., et al. (1992). An Unstable Triplet Repeat in a Gene Related to Myotonic Muscular Dystrophy. *Science* 255 (5049), 1256–1258. doi:10.1126/science.1546326
- Furling, D., Coiffier, L., Mouly, V., Barbet, J. P., St Guily, J. L., Taneja, K., et al. (2001). Defective Satellite Cells in Congenital Myotonic Dystrophy. *Hum. Mol. Genet.* 10 (19), 2079–2087. doi:10.1093/hmg/10.19.2079
- García-Puga, M., Saenz-Antoñanzas, A., Fernández-Torrón, R., Munain, A. L. d., and Matheu, A. (2020). Myotonic Dystrophy Type 1 Cells Display Impaired Metabolism and Mitochondrial Dysfunction that Are Reversed by Metformin. *Aging* 12 (7), 6260–6275. doi:10.18632/aging.103022
- Gramegna, L. L., Giannoccaro, M. P., Manners, D. N., Testa, C., Zanigni, S., Evangelisti, S., et al. (2018). Mitochondrial Dysfunction in Myotonic Dystrophy Type 1. *Neuromuscul. Disord.* 28 (2), 144–149. doi:10.1016/j.nmd.2017.10.007
- Grimberg, A., Coleman, C. M., Burns, T. F., Himelstein, B. P., Koch, C. J., Cohen, P., et al. (2005). p53-Dependent and P53-independent Induction of Insulin-like Growth Factor Binding Protein-3 by Deoxyribonucleic Acid Damage and Hypoxia. *J. Clin. Endocrinol. Metab.* 90 (6), 3568–3574. doi:10.1210/jc.2004-1213
- Hasuike, Y., Mochizuki, H., and Nakamori, M. (2022). Cellular Senescence and Aging in Myotonic Dystrophy. *Int. J. Mol. Sci.* 23 (4), 2339. doi:10.3390/ijms23042339
- Hernandez-Segura, A., Nehme, J., and Demaria, M. (2018). Hallmarks of Cellular Senescence. *Trends Cell Biol.* 28 (6), 436–453. doi:10.1016/j.tcb.2018.02.001
- Johnson, N. E., Butterfield, R. J., Mayne, K., Newcomb, T., Imburgia, C., Dunn, D., et al. (2021). Population Based Prevalence of Myotonic Dystrophy Type 1 Using Genetic Analysis of State-wide Blood Screening Program. *Neurology* 96 (7), e1045–e1053. doi:10.1212/WNL.00000000000011425
- Kaji, K., Ohta, T., Horie, N., Naru, E., Hasegawa, M., and Kanda, N. (2009). Donor Age Reflects the Replicative Lifespan of Human Fibroblasts in Culture. *Hum. Cell* 22 (2), 38–42. doi:10.1111/j.1749-0774.2009.00066.x
- Kasai, S., Shimizu, S., Tatara, Y., Mimura, J., and Itoh, K. (2020). Regulation of Nrf2 by Mitochondrial Reactive Oxygen Species in Physiology and Pathology. *Biomolecules* 10 (2), 320. doi:10.3390/biom10020320
- Kobashigawa, S., Kashino, G., Suzuki, K., Yamashita, S., and Mori, H. (2015). Ionizing Radiation-Induced Cell Death Is Partly Caused by Increase of Mitochondrial Reactive Oxygen Species in normal Human Fibroblast Cells. *Radiat. Res.* 183 (4), 455–464. doi:10.1667/RR13772.1
- Korolchuk, V. I., Miwa, S., Carroll, B., and von Zglinicki, T. (2017). Mitochondria in Cell Senescence: Is Mitophagy the Weakest Link? *EBioMedicine* 21, 7–13. doi:10.1016/j.ebiom.2017.03.020
- Kuilman, T., Michaloglou, C., Mooi, W. J., and Peeper, D. S. (2010). The Essence of Senescence: Figure 1. *Genes Dev.* 24 (22), 2463–2479. doi:10.1101/gad.1971610
- Kumar, A., Kumar, V., Singh, S. K., Muthuswamy, S., and Agarwal, S. (2014). Imbalanced Oxidant and Antioxidant Ratio in Myotonic Dystrophy Type 1. *Free Radic. Res.* 48 (4), 503–510. doi:10.3109/10715762.2014.887847
- Lee, J. E., and Cooper, T. A. (2009). Pathogenic Mechanisms of Myotonic Dystrophy. *Biochem. Soc. Trans.* 37 (Pt 6), 1281–1286. doi:10.1042/BST0371281
- Lofaro, F. D., Boraldi, F., Garcia-Fernandez, M., Estrella, L., Valdivielso, P., and Quagliano, D. (2020). Relationship between Mitochondrial Structure and Bioenergetics in Pseudoxanthoma Elasticum Dermal Fibroblasts. *Front. Cell Dev. Biol.* 8, 610266. doi:10.3389/fcell.2020.610266
- Mahadevan, M., Tsilfidis, C., Sabourin, L., Shutler, G., Amemiya, C., Jansen, G., et al. (1992). Myotonic Dystrophy Mutation: an Unstable CTG Repeat in the 3' Untranslated Region of the Gene. *Science* 255 (5049), 1253–1255. doi:10.1126/science.1546325
- Maier, A. B., and Westendorp, R. G. J. (2009). Relation between Replicative Senescence of Human Fibroblasts and Life History Characteristics. *Ageing Res. Rev.* 8 (3), 237–243. doi:10.1016/j.arr.2009.01.004
- Mavrogomatou, E., Pratsinis, H., Papadopoulou, A., Karamanos, N. K., and Kletsas, D. (2019). Extracellular Matrix Alterations in Senescent Cells and Their Significance in Tissue Homeostasis. *Matrix Biol.* 75–76, 27–42. doi:10.1016/j.matbio.2017.10.004
- McHugh, D., and Gil, J. (2018). Senescence and Aging: Causes, Consequences, and Therapeutic Avenues. *J. Cell Biol.* 217 (1), 65–77. doi:10.1083/jcb.201708092
- Meinke, P., Hintze, S., Limmer, S., and Schoser, B. (2018). Myotonic Dystrophy-A Progeroid Disease? *Front. Neurol.* 9, 601. doi:10.3389/fneur.2018.00601
- Meola, G., and Cardani, R. (2015). Myotonic Dystrophies: An Update on Clinical Aspects, Genetic, Pathology, and Molecular Pathomechanisms. *Biochim. Biophys. Acta (Bba) - Mol. Basis Dis.* 1852 (4), 594–606. doi:10.1016/j.bbadis.2014.05.019
- Mijit, M., Caracciolo, V., Melillo, A., Amicarelli, F., and Giordano, A. (2020). Role of P53 in the Regulation of Cellular Senescence. *Biomolecules* 10 (3), 420. doi:10.3390/biom10030420
- Nakamori, M., Gourdon, G., and Thornton, C. A. (2011a). Stabilization of Expanded (CTG)(CAG) Repeats by Antisense Oligonucleotides. *Mol. Ther.* 19 (12), 2222–2227. doi:10.1038/mt.2011.191
- Nakamori, M., Hamanaka, K., Thomas, J. D., Wang, E. T., Hayashi, Y. K., Takahashi, M. P., et al. (2017). Aberrant Myokine Signaling in Congenital Myotonic Dystrophy. *Cel Rep.* 21 (5), 1240–1252. doi:10.1016/j.celrep.2017.10.018
- Nakamori, M., Pearson, C. E., and Thornton, C. A. (2011b). Bidirectional Transcription Stimulates Expansion and Contraction of Expanded (CTG)(CAG) Repeats. *Hum. Mol. Genet.* 20 (3), 580–588. doi:10.1093/hmg/ddq501
- Nakamori, M., Sobczak, K., Puwanant, A., Welle, S., Eichinger, K., Pandya, S., et al. (2013). Splicing Biomarkers of Disease Severity in Myotonic Dystrophy. *Ann. Neurol.* 74 (6), 862–872. doi:10.1002/ana.23992
- Nakamori, M., Taylor, K., Mochizuki, H., Sobczak, K., and Takahashi, M. P. (2016). Oral Administration of Erythromycin Decreases RNA Toxicity in Myotonic Dystrophy. *Ann. Clin. Transl Neurol.* 3 (1), 42–54. doi:10.1002/acn3.271
- Olive, P. L., and Banáth, J. P. (2006). The Comet Assay: a Method to Measure DNA Damage in Individual Cells. *Nat. Protoc.* 1 (1), 23–29. doi:10.1038/nprot.2006.5
- Otero, B. A., Poukalov, K., Hildebrandt, R. P., Thornton, C. A., Jinnai, K., Fujimura, H., et al. (2021). Transcriptome Alterations in Myotonic Dystrophy Frontal Cortex. *Cel Rep.* 34 (3), 108634. doi:10.1016/j.celrep.2020.108634
- Ozimski, L. L., Sabater-Arcis, M., Bargiela, A., and Artero, R. (2021). The Hallmarks of Myotonic Dystrophy Type 1 Muscle Dysfunction. *Biol. Rev.* 96 (2), 716–730. doi:10.1111/brv.12674
- Passos, J. F., Nelson, G., Wang, C., Richter, T., Simillion, C., Proctor, C. J., et al. (2010). Feedback between P21 and Reactive Oxygen Production Is Necessary for Cell Senescence. *Mol. Syst. Biol.* 6, 347. doi:10.1038/msb.2010.5
- Pendergrass, W., Penn, P., Possin, D., and Wolf, N. (2005). Accumulation of DNA, Nuclear and Mitochondrial Debris, and ROS at Sites of Age-Related Cortical Cataract in Mice. *Invest. Ophthalmol. Vis. Sci.* 46 (12), 4661–4670. doi:10.1167/iovs.05-0808
- Powers, S. K. (2014). Can Antioxidants Protect against Disuse Muscle Atrophy? *Sports Med.* 44 (Suppl. 2), 155–165. doi:10.1007/s40279-014-0255-x
- Rahman, F. A., and Krause, M. P. (2020). PAI-1, the Plasminogen System, and Skeletal Muscle. *Ijms* 21 (19), 7066. doi:10.3390/ijms21197066
- Renna, L. V., Cardani, R., Botta, A., Rossi, G., Fossati, B., Costa, E., et al. (2014). Premature Senescence in Primary Muscle Cultures of Myotonic Dystrophy Type 2 Is Not Associated with P16 Induction. *Eur. J. Histochem.* 58 (4), 2444. doi:10.4081/ejh.2014.2444
- Sabater-Arcis, M., Bargiela, A., Furling, D., and Artero, R. (2020). miR-7 Restores Phenotypes in Myotonic Dystrophy Muscle Cells by Repressing Hyperactivated Autophagy. *Mol. Ther. - Nucleic Acids* 19, 278–292. doi:10.1016/j.omtn.2019.11.012
- Sahashi, K., Tanaka, M., Tashiro, M., Ohno, K., Ibi, T., Takahashi, A., et al. (1992). Increased Mitochondrial DNA Deletions in the Skeletal Muscle of Myotonic Dystrophy. *Gerontology* 38 (1–2), 18–29. doi:10.1159/000213303

- Savkur, R. S., Phillips, A. V., and Cooper, T. A. (2001). Aberrant Regulation of Insulin Receptor Alternative Splicing Is Associated with Insulin Resistance in Myotonic Dystrophy. *Nat. Genet.* 29 (1), 40–47. doi:10.1038/ng704
- Shin, H., Yoo, H. G., Inui, S., Itami, S., Kim, I. G., Cho, A.-R., et al. (2013). Induction of Transforming Growth Factor-Beta 1 by Androgen Is Mediated by Reactive Oxygen Species in Hair Follicle Dermal Papilla Cells. *BMB Rep.* 46 (9), 460–464. doi:10.5483/bmbrep.2013.46.9.228
- Siciliano, G., Mancuso, M., Tedeschi, D., Manca, M. L., Renna, M. R., Lombardi, V., et al. (2001). Coenzyme Q10, Exercise Lactate and CTG Trinucleotide Expansion in Myotonic Dystrophy. *Brain Res. Bull.* 56 (3-4), 405–410. doi:10.1016/s0361-9230(01)00653-0
- Thornell, L.-E., Lindstöm, M., Renault, V., Klein, A., Mouly, V., Ansved, T., et al. (2009). Satellite Cell Dysfunction Contributes to the Progressive Muscle Atrophy in Myotonic Dystrophy Type 1. *Neuropathol. Appl. Neurobiol.* 35 (6), 603–613. doi:10.1111/j.1365-2990.2009.01014.x
- Thornton, C. A. (2014). Myotonic Dystrophy. *Neurol. Clin.* 32 (3), 705–719. doi:10.1016/j.ncl.2014.04.011
- Todorow, V., Hintze, S., Kerr, A. R. W., Hehr, A., Schoser, B., and Meinke, P. (2021). Transcriptome Analysis in a Primary Human Muscle Cell Differentiation Model for Myotonic Dystrophy Type 1. *Ijms* 22 (16), 8607. doi:10.3390/ijms22168607
- Toscano, A., Messina, S., Campo, G. M., Leo, R. D., Musumeci, O., Rodolico, C., et al. (2005). Oxidative Stress in Myotonic Dystrophy Type 1. *Free Radic. Res.* 39 (7), 771–776. doi:10.1080/10715760500138932
- Trapnell, C., Pachter, L., and Salzberg, S. L. (2009). TopHat: Discovering Splice Junctions with RNA-Seq. *Bioinformatics* 25 (9), 1105–1111. doi:10.1093/bioinformatics/btp120
- Turrens, J. F. (2003). Mitochondrial Formation of Reactive Oxygen Species. *J. Physiol.* 552 (Pt 2), 335–344. doi:10.1113/jphysiol.2003.049478
- Usuki, F., and Ishiura, S. (1998). Expanded CTG Repeats in Myotonin Protein Kinase Increase Susceptibility to Oxidative Stress. *Neuroreport* 9 (10), 2291–2296. doi:10.1097/00001756-199807130-00027
- Vassilieva, I., Kosheverova, V., Vitte, M., Kamentseva, R., Shatrova, A., Tsupkina, N., et al. (2020). Paracrine Senescence of Human Endometrial Mesenchymal Stem Cells: a Role for the Insulin-like Growth Factor Binding Protein 3. *Aging* 12 (2), 1987–2004. doi:10.18632/aging.102737
- Vaughan, D. E., Rai, R., Khan, S. S., Eren, M., and Ghosh, A. K. (2017). Plasminogen Activator Inhibitor-1 Is a Marker and a Mediator of Senescence. *Atvb* 37 (8), 1446–1452. doi:10.1161/ATVBAHA.117.309451
- Weng, X., Zhang, X., Lu, X., Wu, J., and Li, S. (2018). Reduced Mitochondrial Response Sensitivity Is Involved in the Anti-apoptotic Effect of D-exmedetomidine P-retreatment in C-ardiomycocytes. *Int. J. Mol. Med.* 41 (4), 2328–2338. doi:10.3892/ijmm.2018.3384
- Wu, C., Liu, X., Wang, Y., Tian, H., Xie, Y., Li, Q., et al. (2013). Insulin-like Factor Binding Protein-3 Promotes the G1 Cell Cycle Arrest in Several Cancer Cell Lines. *Gene* 512 (1), 127–133. doi:10.1016/j.gene.2012.09.080
- Young, M. D., Wakefield, M. J., Smyth, G. K., and Oshlack, A. (2010). Gene Ontology Analysis for RNA-Seq: Accounting for Selection Bias. *Genome Biol.* 11 (2), R14. doi:10.1186/gb-2010-11-2-r14
- Conflict of Interest:** The authors declare that the research was conducted in the absence of any commercial or financial relationships that could be construed as a potential conflict of interest.
- Publisher's Note:** All claims expressed in this article are solely those of the authors and do not necessarily represent those of their affiliated organizations, or those of the publisher, the editors and the reviewers. Any product that may be evaluated in this article, or claim that may be made by its manufacturer, is not guaranteed or endorsed by the publisher.
- Copyright © 2022 Hasuike, Mochizuki and Nakamori. This is an open-access article distributed under the terms of the Creative Commons Attribution License (CC BY). The use, distribution or reproduction in other forums is permitted, provided the original author(s) and the copyright owner(s) are credited and that the original publication in this journal is cited, in accordance with accepted academic practice. No use, distribution or reproduction is permitted which does not comply with these terms.